

---

---

## Compositional and Textural Features of Chromite from the LG6-MG4 Interval in the Western and Eastern Bushveld Complex

Robin D. Lee and Ben Harte

Department of Geology and Geophysics, University of Edinburgh

e-mail: Robin.Lee@glg.ed.ac.uk

### Introduction

Over 800 electron microprobe analyses were made of chromite grains from the LG6, LG7, MG3 and MG4 layers in thin sections from a borehole taken in the Rustenburg area in the western Bushveld, and of chromite grains from the MG4 in thin sections taken from field exposure at Tweefontein, nr. Steelpoort, in the eastern Bushveld. This sequence includes the boundary of the incoming of cumulus plagioclase in the Critical Zone. Analyses were made both of dense chromite (>50% chromite) layers and sublayers, and silicate-dominated sublayers carrying variable amounts of chromite.

K, Na, Mg, Mn, Ni, Ca, Fe, Cr, Al, Ti and Si were analysed for, and these were cast into a 24-cation formula, corrected for  $\text{Fe}^{3+}$  content using the method of Finger (1972). It is noted that in this method  $\text{Fe}^{3+}$  and  $\text{Fe}^{2+}$  contents may be significantly affected by errors in analyses of the other elements.  $\text{R}^{4+}$ , dominated by  $\text{Ti}^{4+}$ , and  $\text{R}^{+}$ , dominated by  $\text{Na}^{+}$ , contents reach a maximum of 0.422 and 0.050 cations respectively. It is surmised that these cations are accommodated via the substitutions  $2(\text{R}^{3+}) \rightarrow \text{R}^{2+}\text{R}^{4+}$  and  $\text{R}^{2+}\text{R}^{3+} \rightarrow \text{R}^{+}\text{R}^{4+}$ . In general, individual chromite grains show no zoning.

### Broad compositional trends

A plot of Mg against  $\text{Fe}^{2+}$  (Fig. 1) shows the data to be well constrained between  $\text{sum}=7.9$  and  $\text{sum}=8.3$  cations. Analyses from the MG4B layer at Rustenburg have higher total Mg,  $\text{Fe}^{2+}$  contents than those from layers below, which show the general trend of enrichment in  $\text{Fe}^{2+}$  at the expense of Mg from LG6 to MG3. There are reversions to higher Mg/ $\text{Fe}^{2+}$  ratios at the top of the LG6, in the LG7, at the top of the MG3, and within the MG4. The Ti contents (Fig. 2) of the chromites increase from an average of 0.16 cations at the LG6 to between 0.19 and 0.42 cations at the MG4B. This combination of high Ti contents and a reversion to higher Mg/ $\text{Fe}^{2+}$  ratios at the MG4B are suggestive of the combination of an evolved residual magma with an influx of primitive basic magma. The MG4B and MG4C layers at Tweefontein show a similar pattern, with the

MG4B showing low Mg# and Ti enrichment. The MG4C reverts to higher Mg# and low Ti content.

Plots of Cr and Al against Mg# ( $\text{Mg}/(\text{Mg}+\text{Fe}^{2+})$ ) show that Cr content has a broad antipathetic relationship with Mg# whereas Al content has a sympathetic relationship with Mg#. Cr contents lie on the same trend at both locations, but at Tweefontein Al contents follow a lower, parallel trend to Rustenburg for the same Mg#. Thus Al# ( $\text{Al}/(\text{Al}+\text{Cr})$ ) has a sympathetic relationship with Mg# (Fig. 4). At Rustenburg, the LG6 has the highest Al# (up to 0.43), and this decreases up to the top of the layer. There is a reversion to higher values at the LG7, then a decrease at the base of the MG3. The middle of the MG3 has similar values to the LG7. The base of the MG4B has the lowest Al# (0.20 to 0.30), but the main MG4B reverts to 0.29 to 0.33. The MG4A samples at Tweefontein show a similar reversal.

$\text{Fe}^{3+}$  contents (Fig. 3) in the Rustenburg core from the LG6 average 1.0 cations; from the LG7 to the base of the MG4B the average is 1.3 cations. In the MG4B proper  $\text{Fe}^{3+}$  contents revert to an average of 1.0 cations. Samples from the Tweefontein exposure have elevated  $\text{Fe}^{3+}$  contents varying from 1.2 to 3.6 cations. The Fe ratio ( $\text{Fe}^{3+}/(\text{Fe}^{3+}+\text{Fe}^{2+})$ ) of the chromites shows a similar trend to the  $\text{Fe}^{3+}$  contents, except that the base of the MG4B at Rustenburg shows similar ratios to the LG6, and not the LG7-base of the MG4B interval.

### Compositional trends and textural features within samples

Sections that are sublayered and show small-scale modal and textural heterogeneities, i.e. variations in the modes of chromite, pyroxene and plagioclase, show common features on a plot of Al#-Mg#. Where chromite is the dominant phase, and especially where it shows annealed, polygonal texture, the range of Al# and Mg# is small compared to where cumulus pyroxene is a major, or the dominant, phase. Here, Mg#s are trailed out to lower values, with little change in Al#. This is pronounced in the LG6, where modal sublayering is pronounced. This greater spread of compositions in the chromite-poor sublayers may represent subsolidus equilibration, postcumulus equilibration,

or simply the later growth of some chromite grains – which in pyroxene-rich sublayers sometimes have an interstitial appearance. Less commonly, chromites in pyroxene-rich sublayers may have

higher Mg# and Al# than those in chromite-rich sublayers. Significant plagioclase cements the LG7 and base of the MG3, and these show similar patterns.

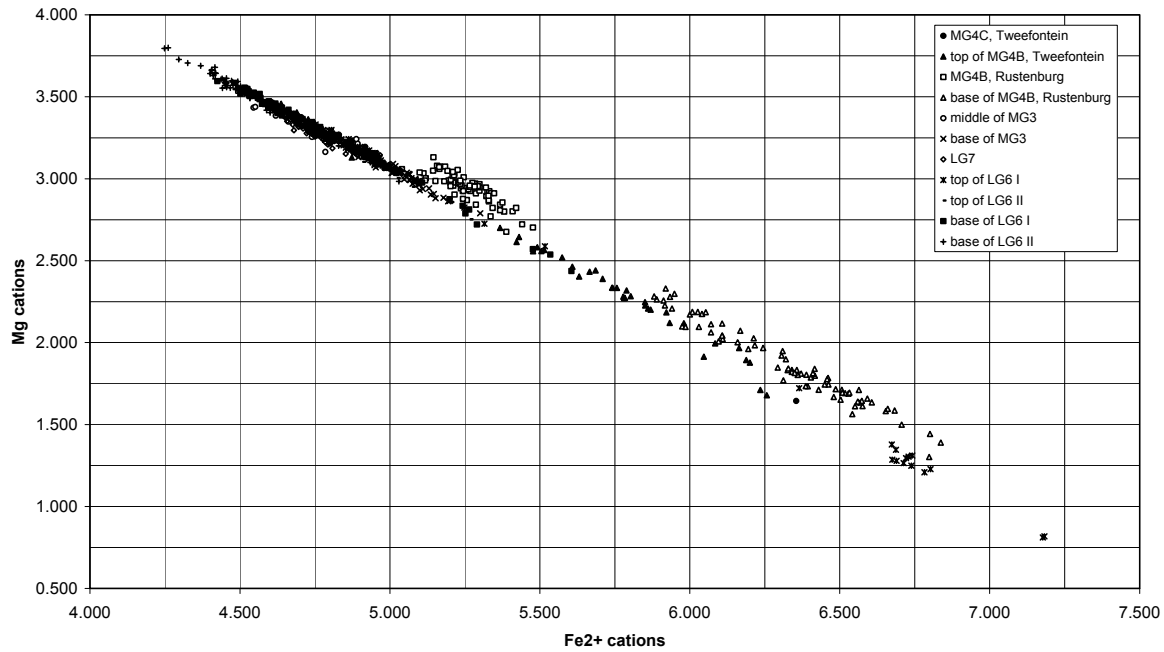


**Figure 1.** Mg vs.  $Fe^{2+}$ .

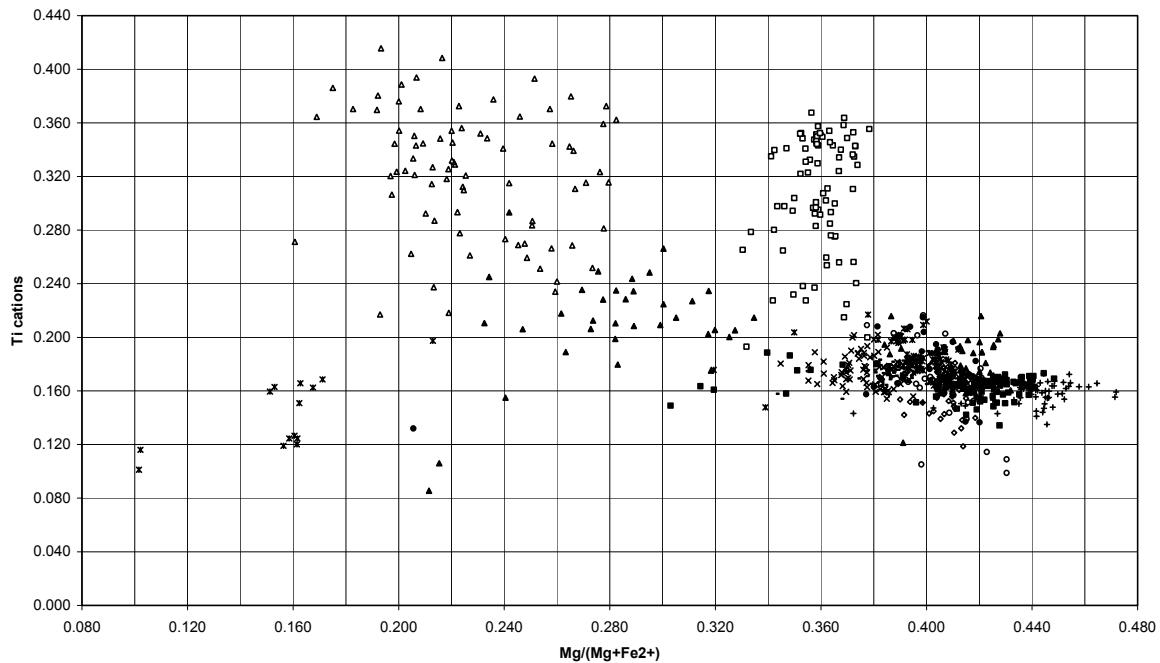


**Figure 2.** Ti cations vs. Mg number.

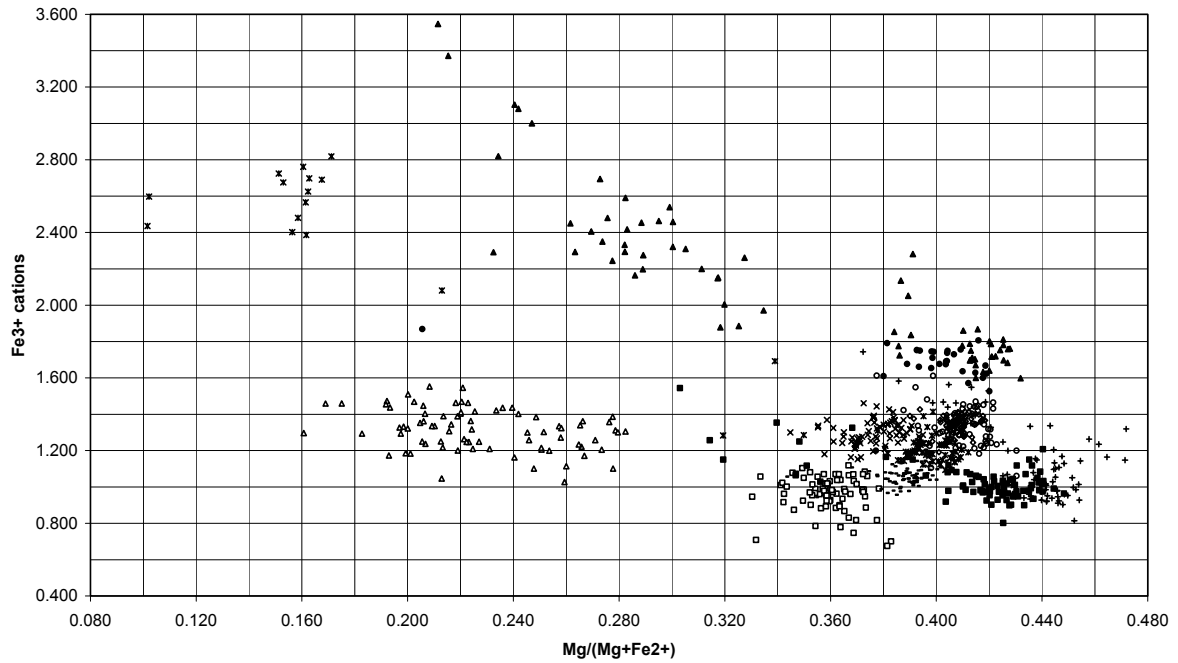


**Figure 3.** *Fe<sup>3+</sup> cations vs. Mg number.*

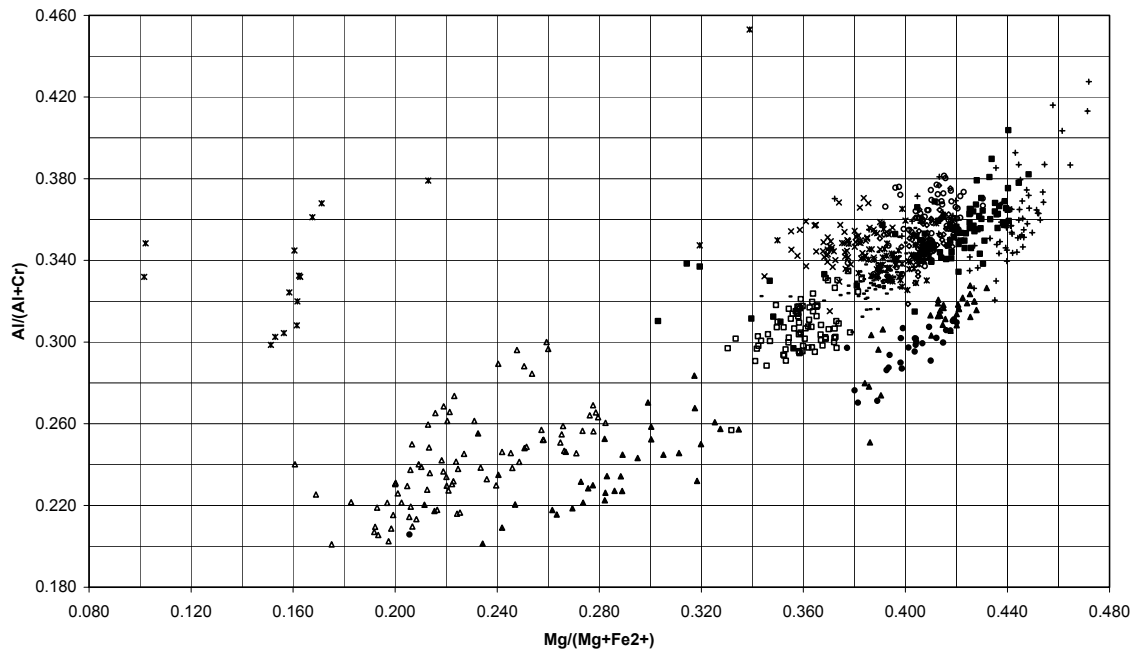


**Figure 4.** *Al/(Al + Cr) vs. Mg number.*

A section from the middle of the MG3 contains a thin band of adcumulus plagioclase between two dense chromitites. The two chromitites sit on different trends on an Al#-Mg# plot, with the upper chromitite at higher Mg# and

lower Al#. A drop in Al# may be explained by the removal of Al from the crystallizing liquid into the plagioclase in the adcumulate below, but plagioclase is unlikely to alter Mg#. Hence the upper layer may be of a different, more primitive

origin to the lower layer, as it also has lower Fe<sup>3+</sup> content than the lower layer.

The MG4 does not follow the previous trends. At Rustenburg, the base of the MG4B is composed of cumulus pyroxene with interstitial plagioclase, sometimes extending into plagioclase-rich pools. Chromite is mainly found in the interstices, but there is good evidence that the pyroxenes have overgrown chromites, which retain a thin contact with the interstitial plagioclase. In areas where chromite is trapped between cumulus pyroxene it appears that grains of chromite have been overgrown to give them an interstitial appearance. The middle of the MG3 is a dense chromitite cemented by pyroxene and plagioclase – here chromites cemented by plagioclase have lower Al# than those in pyroxene, and chromites cemented by pyroxene trail off to lower values of Mg#, with some at higher Mg#. This is consistent with subsolidus equilibration, but may alternatively represent postcumulus equilibration, assuming that cementation by pyroxene was earliest. Annealed patches of chromite have restricted Mg# and Al#.

The sublayers of the MG4 at Tweefontein may not be directly correlable with those at Rustenburg. A section across the chromitite/pyroxene cumulate contact at the top of the MG4B layer shows that chromites in the chromitite layer have well constrained Mg# and Al#; chromites in the pyroxene cumulate are usually present in interstitial plagioclase, and have distinct compositions with lower Mg# and Al#. Also, some grains in the pyroxene cumulate appear to have been picked up from the chromitite and equilibrated to slightly lower Mg# and Al#. The section from the MG4C contains a pegmatoid between two dense chromitites – chromite in the chromitite has well-constrained Mg# and Al#, whereas chromite in the pegmatoid trails off to lower Mg# and Al#, but with several grains at higher Mg# and Al#. This is consistent with previous observations.

#### Acknowledgements

To Dr Peter Hill, University of Edinburgh, for his guidance on the electron microprobe; to Wikus Jordaan and Martin Köhler at the Council for Geoscience, SA, for their invaluable help; and to Manie Swart and Syd Absalom at Samancor Ltd., for their assistance at the Tubatse Chrome Mine, Tweefontein.

#### References

- Barnes, S.J., 1986, The distribution of chromium among orthopyroxene, spinel and silicate liquid at atmospheric pressure: *Geochim. Cosmochim. Acta*, v. 50, p. 1889-1909.
- Barnes, S.J., and Roeder, P.L., 2001, The Range of Spinel Compositions in Terrestrial Mafic and Ultramafic Rocks: *J. Pet.*, v. 42, p. 2279-2302.
- Cameron, E.N., and Desborough, G.A., 1969, Occurrence and Characteristics of Chromite Deposits – Eastern Bushveld Complex: *Econ. Geol. Monographs*, no. 4, p. 23-40.
- Hulbert, L.J., and Von Gruenewaldt, G., 1985, Textural and Compositional Features of Chromite in the Lower and Critical Zones of the Bushveld Complex South of Potgietersrus: *Econ. Geol.*, v. 80, p. 872-895.
- Irvine, T.N., 1974, Crystallization sequences in the Muskox intrusion and other layered intrusions – II. Origin of chromitite layers and similar deposits of other magmatic ores: *Geochim. Cosmochim. Acta*, v. 39, p. 991-1020.
- Irvine, T.N., 1977, Origin of chromitite layers in the Muskox intrusion and other stratiform intrusions: A new interpretation: *Geology*, v. 5, p. 273-277.
- Roeder, P.L., and Reynolds, I., 1991, Crystallization of Chromite and Chromium Solubility in Basaltic Melts: *J. Pet.*, v. 32, p. 909-934.
- Scoon, R. N., and Teigler, B., 1994, Platinum-Group Element Mineralization in the Critical Zone of the Western Bushveld Complex: Sulfide Poor-Chromitites below the UG-2: *Econ. Geol.*, v. 89, p. 1094-1121.
- Teigler, B., Eales, H.V., and Scoon, R.N., 1992, The cumulate succession in the Critical Zone of the Rustenburg Layered Suite at Brits, western Bushveld Complex: *South African J. Geol.*, v. 95, p. 17-28.
- Teigler, B., and Eales, H.V., 1993, Correlation between chromite composition and PGE mineralization in the Critical Zone of the western Bushveld Complex: *Mineral. Deposita*, v. 28, p. 291-302.